Available online at www.sciencedirect.com
SCIENCE DIRECT
Journal of Power Sources 146 (2005) 180–184
JOURNAL OF POWER SOURCES
www.elsevier.com/locate/jpowsour

Nano-structured SnO_2-carbon composites obtained by in situ spray pyrolysis method as anodes in lithium batteries

Ling Yuan *, K. Konstantinov, G.X. Wang, H.K. Liu, S.X. Dou

Institute of Superconducting and Electronic Materials University of Wollongong, NSW 2522, Australia

Available online 24 May 2005

Abstract

In this paper, we report on a series of SnO_2-carbon nano-composites synthesized by in situ spray pyrolysis of a solution of $SnCl_2{\cdot}2H_2O$ and sucrose at 700 °C. The process results in super fine nanocrystalline SnO_2, which is homogeneously distributed inside the amorphous carbon matrix. The SnO_2 was revealed as a structure of broken hollow spheres with porosity on both the inside and outside particle surfaces. This structure promises a highly developed specific surface area. X-ray diffraction (XRD) patterns and transmission electron microscope (TEM) images revealed the SnO_2 crystal size is about 5–15 nm. These composites show a reversible lithium storage capacity of about 590 mAh g^{-1} in the first cycle. The discharge curve of the composite indicates that lithium is stored in crystalline tin, but not in amorphous carbon. However, the conductive carbon matrix with high surface area provides a buffer layer to cushion the large volume change in the tin regions, which contributes to the reduced capacity fade compared to nonacrystalline SnO_2 without carbon.

Keywords: Lithium-ion; Anodes; SnO_2; Composite; Carbon; Tin

1. Introduction

Since FUJI Photofilm published patents [1,2] for the use of tin-based composite oxide (TCO) as an alternative anode material for lithium-ion batteries in 1995, a lasting interest in tin alloys and compounds has grown. As possible anodes for next generation lithium-ion batteries, tin oxide based materials show great promise for their high storage capacity [3]. However, as is always observed, the significant capacity fading of these anodes has undermined the advantage.

Many efforts have been devoted to attempts to reduce the capacity fading. Generally, two approaches have been attempted:

(1) A number of nano-structured SnO_2 materials have been synthesized by a variety of methods such as sol–gel templating [4,5] and reverse microemulsion [6]. The nano-structure ensures that the Sn region is small enough initially to get a fast diffusion of lithium-ions into the electrode, and prevents the Sn regions from aggregating.

(2) Different matrixes which have electronic and ionic conductivity throughout the electrode have been investigated to accommodate the large volume changes have been searched. Recently, the search for a suitable matrix has been focused on carbonaceous materials which can reduce the fading in capacity to some extent [3,7–10].

Following these two approaches, we aim to synthesize a nano-structured SnO_2 material, and search for a suitable matrix to accommodate the impressive volume changes. In the present study, the spray pyrolysis technique was applied to synthesize in situ a series of SnO_2-carbon nano-composites at 700 °C. The spray pyrolysis in situ process ensures that the chemical reaction is completed during very short time, preventing the crystals from growing larger.

A solution of $SnCl_2{\cdot}2H_2O$ and sucrose has been used as a spray precursor. The process results in super fine nanocrystalline SnO_2, which is distributed homogeneously inside the amorphous carbon matrix. This paper reports on the formation of the composites and their electrochemical properties as anodes in lithium-ion batteries.

* Corresponding author. Tel.: +61 2 4221 3017; fax: +61 2 4221 5731.
E-mail address: ly93@uow.edu.au (L. Yuan).

0378-7753/$ – see front matter © 2005 Elsevier B.V. All rights reserved.
doi:10.1016/j.jpowsour.2005.03.008

2. Experimental

The spray precursors were prepared by mixing saturated aqueous sucrose solutions with tin(II) chloride dihydrate (Aldrich, 98%) 1 M ethanol solution, in $SnCl_2{\cdot}2H_2O$/sucrose in weight ratios of 100:0, 60:40, 40:60, and 10:90, respectively. The SnO_2 pure sample and SnO_2-carbon composites were obtained in situ using a vertical type of spray pyrolysis reactor at 700 °C.

Powder X-ray diffraction (1730 X-ray diffractometer) using Cu Kα radiation was employed to identify the crystalline phase of the synthesized materials. The solid morphologies of the resulting composites were observed using a scanning electron microscope (SEM) (Leica/Cambridge Steroscan 440). Transmission electron microscope (TEM) and high resolution (HR) TEM images were obtained from a Philips M12 and JEOL F3000 microscope, respectively. Differential thermal and thermo-gravimetric (DTA–TG) analysis was carried out by using Setaram 92 equipment. The Brunauer–Emmett–Teller (BET) specific surface area was measured by a Quantachrome Nova 1000 gas sorption analyser. The electrochemical characterisations were performed using R2032 coin cells. The anode was prepared by mixing SnO_2 or SnO_2-carbon composites with 10 wt.% carbon black and 10 wt.% polyvinylidene fluoride (PVDF) binder; then drops of *N*-methyl-2-pyrrolidinone (NMP) were added to form a slurry with appropriate viscosity. The mixture was then used to coat copper foils to a mass loading of about 1 mg after drying (at 140 °C) and compaction (at rate of 150 kg cm^{-2}). Each coated electrode was assembled into a test coin cell in an argon-filled glove-box (Mbraun, Unilab, USA). The counter electrode was Li metal and the electrolyte was 1 M $LiPF_6$ dissolved in a 50:50 (v/v) mixture of ethylene carbonate (EC) and dimethyl carbonate (DMC) provided by MERCK KgaA, Germany. The cells were charge–discharged at the constant current density of 0.04 mA cm^{-2} and within the voltage range of 0.05–1.25 V at room temperature, to determine the electrochemical characteristics. Cyclic voltammograms (CV) measurements were carried out using an EG&G potentiostat (model M362) at a scanning rate of 0.1 mV s^{-1}.

3. Results and discussion

3.1. Characterization and morphology

The amount of tin in the samples was determined by thermogravimetric analysis (TGA) in air. The precursors of $SnCl_2{\cdot}2H_2O$/sucrose in weight ratios of 100:0, 60:40, 40:60, and 10:90 resulted in SnO_2 without carbon and SnO_2-carbon composites containing 89, 65, and 49 wt.% SnO_2, respectively. Scanning electron micrographs of the products from the spray pyrolysis process are shown in Fig. 1. All the samples were morphologically alike, presenting a structure resembling broken hollow spheres with porosity on both the inside and the outside particle surfaces (Fig. 1(d)). Fig. 2 shows the X-ray diffraction patterns of samples synthesized by the spray pyrolysis method. All diffraction patterns show the SnO_2 phase as indexed. The SnO_2 without carbon (Fig. 2(a)) and SnO_2-carbon composites Fig. 2(b)–(d) are revealed as crystalline structures, however, the carbon in the composites was not identified by the XRD diffraction pattern, which indicates the amorphous structure of the carbon. The broad diffraction peaks indicate that the SnO_2 is in the form of small

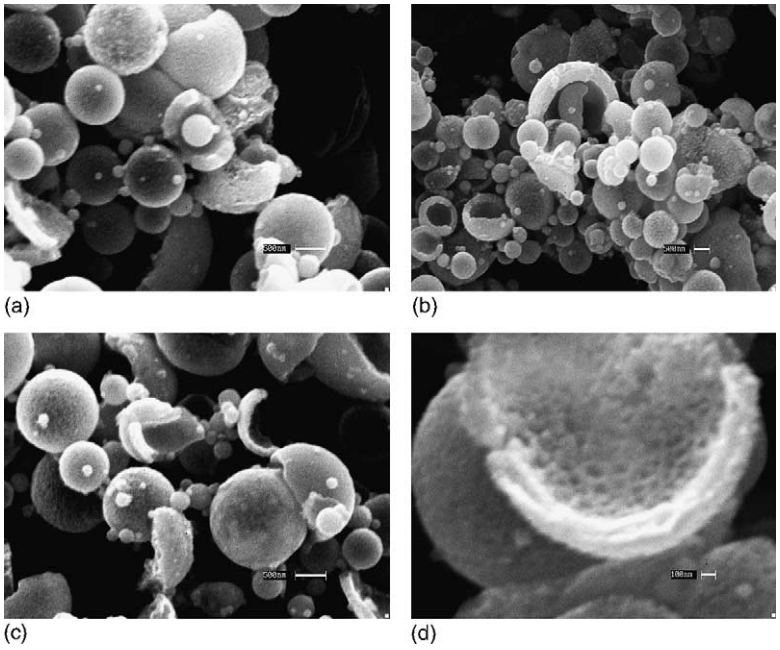

Fig. 1. SEM images of (a) SnO_2 without carbon, and SnO_2-carbon composites from the spray pyrolysis process; (b) with SnO_2 contents of 89 wt.%; (c) 65 wt.%; (d) 49 wt.% (enlarged image).

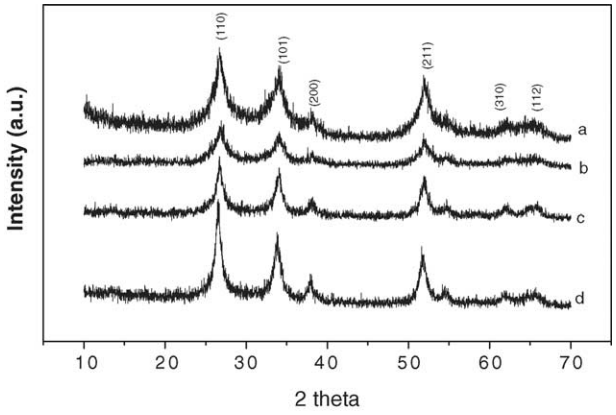

Fig. 2. X-ray powder patterns of sprayed samples: (a) SnO_2 without carbon and SnO_2-carbon composites; (b) $89SnO_2{\cdot}11C$; (c) $65SnO_2{\cdot}35C$; and (d) $49SnO_2{\cdot}51C$.

crystals in all samples. The grain size for the sprayed samples calculated using the Scherrer formula is in the range of 5–15 nm.

The patterns (Fig. 2(b)–(d)) also show that the peak intensities increase slightly with increasing carbon content in the composites. Since the spray pyrolysis in situ process causes the chemical reaction to be completed within a very short time, there are large amounts of heat released as the sucrose decomposes, which results in the local temperature increasing very quickly. The more sucrose added in the precursor, the higher the local temperature could go, therefore, the more crystalline SnO_2 could form under this higher temperature.

The TEM and HRTEM images shown in Fig. 3 confirmed the calculated SnO_2 crystal size of 5–15 nm. The crystalline SnO_2 grains are surrounded by amorphous carbon. These images demonstrated the nanostructure of the composites containing crystalline SnO_2 which is distributed homogeneously inside the amorphous carbon matrix. The morphological structure of the samples suggests a high specific surface area. Brunauer–Emmett–Teller (BET) specific surface area measurements were conducted, and the results are shown in Table 1. We found that with the carbon content increasing, the specific surface area increased from 20 $m^2\ g^{-1}$ (0 wt.% carbon) to 145 $m^2\ g^{-1}$ (51 wt.% carbon). Compared with 7 $m^2\ g^{-1}$ for the commercial SnO_2, there is a significant improvement in the surface area.

Table 1
Results from BET measurement

Samples	Content of carbon (wt.%)	Specific surface area ($m^2\ g^{-1}$)
Commercial SnO_2 (Aldrich, 99%)	0	7.1525
Sprayed SnO_2	0	20.3547
$89SnO_2{\cdot}11C$	11	73.6849
$65SnO_2{\cdot}35C$	35	107.9626
$49SnO_2{\cdot}51C$	51	145.3734

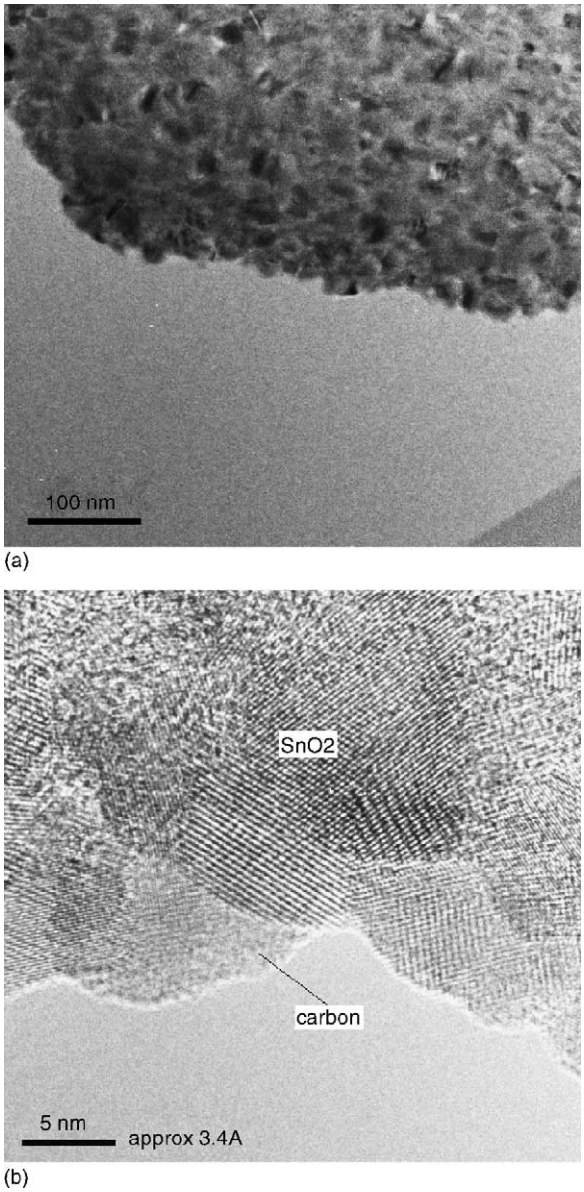

Fig. 3. TEM (a) and HRTEM (b) images of $65SnO_2{\cdot}35C$ composite.

3.2. Electrochemical properties

It is believed that SnO_2 reacts with lithium in a two-step process as follow [11]:

$$SnO_2 + 4Li^+ + 4e^- \rightarrow Sn + 2Li_2O \quad (1)$$

$$Sn + \chi Li^+ + \chi e^- \leftrightarrow Li_\chi Sn \quad 0 \le \chi \le 4.4 \quad (2)$$

Firstly, the irreversible conversion of SnO_2 results in the formation of metallic tin regions dispersed within a Li_2O matrix; then the lithium alloying/de-alloying with Sn provides the reversible lithium storage capacity of the material [12]. A large volume change occurs in the Sn regions during the lithium insertion and extraction reactions. Even if the Li_2O matrix slows the aggregation process, it does not prevent it. [13] Consequently, the mechanical stresses lead to

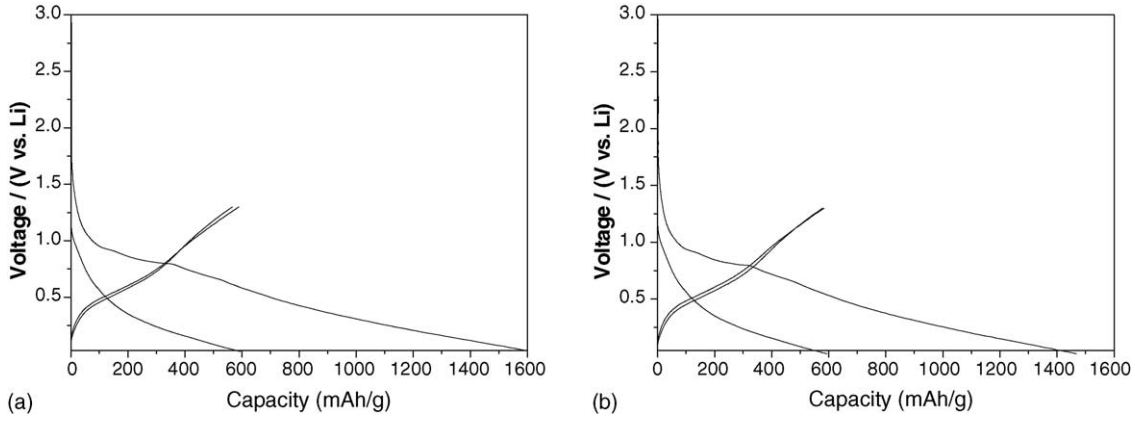

Fig. 4. The first and second discharge and charge curves of (a) nanostructured SnO_2 without carbon and (b) $65SnO_2{\cdot}35C$ composite at 0.04 mA cm^{-2}.

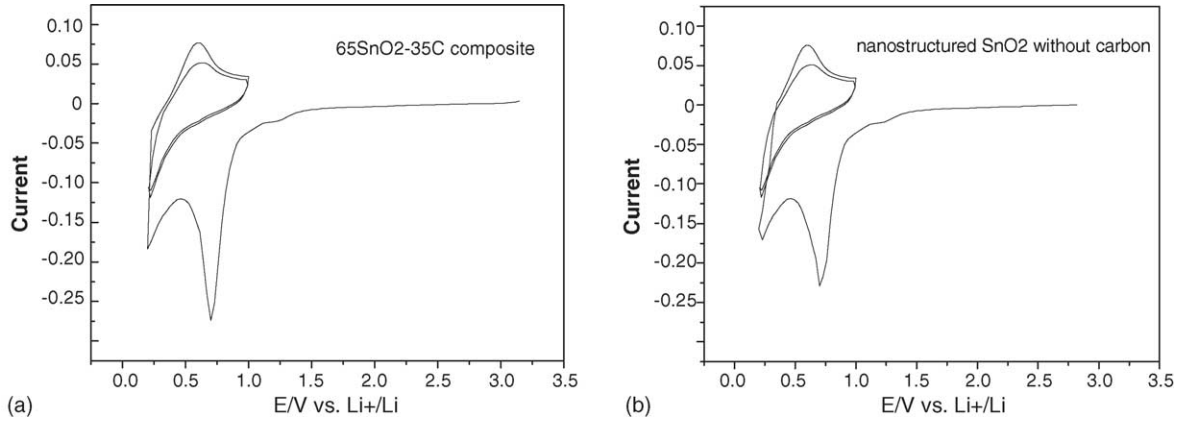

Fig. 5. Cyclic Voltammograms for (a) a nanostructured $65SnO_2{\cdot}35C$ composite electrode and (b) a nanostructured SnO_2 without carbon electrode. Scan rate 0.1 mV s^{-1}.

the electrode cracking and losing electrical contacts between particles, which cause a sharp decrease in capacity.

The specific capacity and cycling stability of nanostructured SnO_2 and SnO_2-carbon composites electrodes were measured by constant current charge/discharge testing. Fig. 4 shows the first and second charge and discharge curves of the SnO_2 and $65SnO_2{\cdot}35C$ composite at 0.04 mA cm^{-2} between 0 and 1.25 V. The discharge curves of SnO_2 and $65SnO_2{\cdot}35C$ composite are fairly similar in appearance, which confirms that only tin in the composite contributes to the electrochemical capacity. There is a plateau in the charging curves below 1 V, which shows SnO_2 and SnO_2-carbon composite working in the low-potential range (0–1.2 V versus Li/Li^+). This plateau is believed to correspond to the formation of Li_2O and Sn in Eq. (2). The first reversible lithium storage capacity of the SnO_2 and the $65SnO_2{\cdot}35C$ composite is 589 and 585 mAh g^{-1}, respectively.

Fig. 5 shows cyclic voltammograms for nanostructured SnO_2 and $65SnO_2{\cdot}35C$ composite electrodes at a scan rate of 0.1 mV s^{-1}. The CV curves for both SnO_2 and $65SnO_2{\cdot}35C$ composite electrodes clearly indicate the irreversible reaction during the first discharge with a reduction peak at 0.7 V. During the following cycles, this peak disappears and only the peaks at low potential (<0.5 V) corresponding to the Li–Sn alloy formation are observed.

Fig. 6 compares the discharge capacity versus the number of charge/discharge cycles for the nano-structured

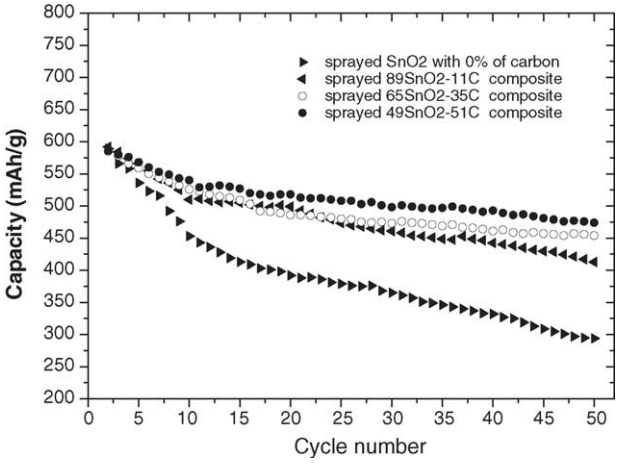

Fig. 6. Discharge capacity vs. cycle number for the potential range from 0.1 to 1.3 V for the nanostructured SnO_2 and SnO_2-carbon composites.

SnO_2 and SnO_2-carbon composites electrodes. After 50 charge–discharge cycles, SnO_2, $89SnO_2{\cdot}11C$, $65SnO_2{\cdot}35C$, and $49SnO_2{\cdot}51C$ electrodes remained at 46, 66, 77, and 81%, respectively, of their initial discharging capacity. The composites show a significantly improved cycle-life performance compared with SnO_2 without carbon.

We believe that the nanostructure of the sprayed powder and the conductivity and ductility of the carbon matrix are responsible for the good cycle-life performance observed. Firstly, the nano-structured crystalline SnO_2 ensures that the Sn region is small enough initially to promote a fast diffusion of lithium-ion into the electrode, preventing the Sn regions from aggregating. Moreover, the composites made by the spray pyrolysis method have a more uniform distribution of SnO_2 in the carbon than what could be obtained by mechanical milling. The SnO_2 particles are trapped and separated by the carbon, not just mechanically mixed with or dispersed in carbon. The carbon matrix provides an effective cushion against the specific volume changes in the tin regions.

4. Conclusions

A series of SnO_2-carbon nano-composites were obtained by in situ spray pyrolysis of a mixed solution of $SnCl_2{\cdot}2H_2O$ and sucrose at 700 °C. The process results in super fine nanocrystalline SnO_2, which is distributed homogeneously inside the amorphous carbon matrix. The SnO_2 presents a structure resembling broken hollow spheres, which is porous on both the inside and outside particle surfaces. This structure promises a highly developed specific surface area. The XRD patterns and TEM images revealed the SnO_2 crystal size is about 5–15 nm. The discharge curves of nanostrucuted SnO_2 without carbon and SnO_2-carbon composite electrodes are fairly similar in appearance, which confirms that only tin in the composite contributes to the electrochemical capacity. The SnO_2-carbon composites showed a significantly improved cycle-life performance compared with SnO_2 without carbon. We suggest that the nano-structure of crystalline SnO_2 prevents the Sn regions from aggregating to some extent, and that the presence of the carbon matrix provides an effective cushion against the specific volume changes in the tin regions.

Acknowledgements

This work was financially supported by the Australian Research Council through an ARC linkage project (LP0219309) with industry partners: Sons of Gwalia Ltd. and OMG. The authors sincerely thank Dr. Zaiping Guo for valuable discussion and Dr. Tania Silver for help with the editing.

References

[1] Y. Idota, US Patent 5478671 (1995).
[2] H. Tomyama, Jpn. Patent 07-029608 (1995).
[3] Y. Idota, A. Matsufuji, Y. Mackawa, T. Miyasaka, Science 276 (1997) 1395.
[4] N. Li, C.R. Martin, B. Scrosati, Electrochem. Solid State Lett. 3 (7) (2000) 316.
[5] N. Li, C.J. Patrissi, G. Che, C.R. Martin, J. Electrochem. Soc. 147 (2000) 2044.
[6] Y. Wang, J.Y. Lee, B.H. Chen, Electrochem. Solid State Lett. 6 (1) (2003) A19.
[7] J.Y. Lee, R.F. Zhang, Z.L. Liu, Electrochem. Solid State Lett. 3 (2000) 167.
[8] J.Y. Lee, R.F. Zhang, Z.L. Liu, J. Power Sources 90 (2000) 70.
[9] J. Read, D. Foster, J. Wolfenstine, W. Behl, J. Power Sources 96 (2001) 277.
[10] J. Santos-Pena, T. Brousse, D.M. Schleich, Solid State Ionics 135 (2000) 87.
[11] I.A. Courtney, J.R. Dahn, J. Electrochem. Soc. 144 (1997) 2045.
[12] I.A. Courtney, J.R. Dahn, J. Electrochem. Soc. 144 (1997) 2943.
[13] I.A. Courtney, W.R. McKinnon, J.R. Dahn, J. Electrochem. Soc. 146 (1999) 59.